Article

Bioaerosols as Evidence of Atmospheric Circulation Anomalies over the Okhotsk Sea and Shantar Islands in the Late Glacial–Holocene

Nadezhda Razjigaeva [1,*], **Larisa Ganzey** [1], **Tatiana Grebennikova** [1], **Vladimir Ponomarev** [2], **Ludmila Mokhova** [1], **Vladimir Chakov** [3] **and Mikhail Klimin** [3]

[1] Pacific Geographical Institute FEB RAS, Radio St., 7, 690041 Vladivostok, Russia; lganzey@mail.ru (L.G.); tagrebennikova@mail.ru (T.G.); pvi711@yandex.ru (L.M.)

[2] V.I. Il'ichev Pacific Oceanological Institute FEB RAS, Baltiyskaya, 43, 690041 Vladivostok, Russia; tigpaleo@mail.ru

[3] Institute of Water and Ecological Problems FEB RAS, Dikopoltsev St., 56, 680000 Khabarovsk, Russia; chakov@ivep.as.khb.ru (V.C.); m_klimin@bk.ru (M.K.)

* Correspondence: nadyar@tigdvo.ru; Tel.: +7-924-237-89-81

Abstract: Allochthonous biofossil distribution in the blanket peat bog of Bolshoy Shantar Island was used to analyze atmospheric circulation anomalies in the north-western Okhotsk Sea over the last 12.6 ka. The main aim of this study was to determine periods of intensification of deep cyclones and extreme storms. The composition of bioaerosols is significantly influenced by atmospheric zonal and meridional transport anomalies associated with anomalies of the monsoon system of Northeast Asia, atmospheric fronts and cyclone trajectories. Marine diatoms enter the peatland from the sea during extreme storms and record the passage of sea cyclones in the autumn-winter, whereas the distribution of allochthonous pollen indicates the intensity of continental cyclones. We used *Pinus pumila* pollen as an indicator of heavy snowfalls and winter cyclone activity. Fifteen phases of extreme storms were identified. Changes in ice coverage also played an important role in bioaerosol emission. During cold periods, emissions of bioaerosols mainly occurred in the open sea, whereas during warm periods, emissions occurred near the coast. The recurrence and intensity of cyclones during the cold seasons depends on displacement of the Siberian High and Aleutian Low. Periods of continental cyclones intensified in spring-summer and coincided with periods of active winter cyclogenesis.

Keywords: cyclogenesis; extreme storms; Siberian High; Aleutian Low; blanket peatbog; allochthonous biofossils (pollen and diatoms)

1. Introduction

Bioaerosols are aerosols that include biological material and can be transported over hundreds to thousands of kilometers. Viruses, bacteria, pollen, spores of non-vascular plants and fungi, mold, diatoms, remains of insects and plants, other bioparticles, and endotoxins can be transported as aerosols [1]. Particle sizes range from nanometers up to tens or even hundreds of micrometers. In boreal regions, the concentration of bioaerosols varies from 3 to 6 µg m^{-3} and can reach 30–60% of the total aerosol material [2,3]. During the growing season, bioaerosols mainly consist of plant pollen, which, despite its large size (10–100 µm), can be transported by air currents, over 1000 km [4].

An important source of bioaerosols is the marine environment. Tiny bubbles form on the sea surface during high winds and storms, and then burst when the formation grows to a large number of drops. Upon drying, these drops turn into salt particles (less than 0.1 µm in size) that can enter the atmosphere as aerosols [1,5]. During this time, microorganisms such as cyanobacteria and phytoplankton (e.g., dinoflagellates, diatoms) can enter the aerosols.

Marine aerosols enriched with sea salt increase the chlorine (Cl) content in snow, which has been previously seen on the eastern macroslope of the Sikhote-Alin Mountains (south of the Russian Far East), over 30 km from the coast of the Japan Sea [6]. Marine aerosols increase the content of sulfate (SO_4) and calcium (Ca) in atmospheric precipitation. The highest concentrations of SO_4 and Ca have been found on Sakhalin near the Aleksandrovsk meteorological station, located 1 km from the Tatar Strait (the Japan Sea), as well as in Poronaysk (the Okhotsk Sea) and Petropavlovsk-Kamchatsky (the Bering Sea) [6]. A significant role in the transport of marine aerosols was oceanic spray carried by strong winds during storms [6].

Since aerosols are nuclei of water-vapor condensation, they play a significant role in cloud formation [1,6–10]. Bioparticles, depending on their hygroscopic and condensation properties, can also serve as condensation nuclei in the atmosphere and affect the formation of clouds [11]. Bioaerosols can possibly disperse bioactive material over long distances (biomarkers) and can be a source of allergies [12], biological pollution, or a method of pathogen infection [1]. The study of bioaerosols composition can also be used to reconstruct past atmospheric circulation anomalies.

The purpose of this study was to determine the periods of frequent and strong storms and the peculiarities of atmospheric processes in the Holocene based on the composition of allochthonous biofossils (pollen and diatoms) in a watershed peat bog. We also aimed to estimate the possible distances of biomaterial transfer during different periods of the Holocene. The Shantar Islands were chosen as the location of the study because the composition of allochthonous biofossils at this location is significantly influenced by anomalies of zonal and meridional transport in the atmosphere, which are associated with the monsoon system of Northeast Asia, atmospheric fronts and cyclone tracks. Strong winds from various directions and high storm activity are typical features of atmospheric processes over the Okhotsk Sea adjacent to these islands.

2. Regional Settings

The Shantar Islands are located in the western part of the Okhotsk Sea (Figure 1). The depths of the straits separating the islands from the continent vary from 24 to 44 m (Lindholm Strait). The distance from Bolshoy Shantar Island to the continent reaches ~30 km.
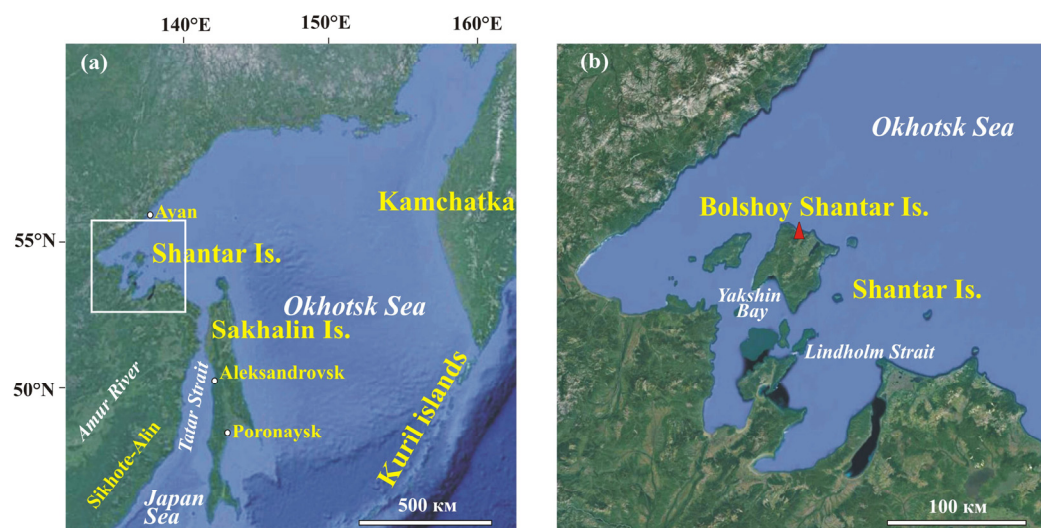
Figure 1. Study area: (**a**) Okhotsk Sea and location of study area; (**b**) Shantar Islands and position of study site (red triangle).

The islands are part of the Priokhotsk monsoon climatic region [13]. The air circulation is determined by the interaction of the Siberian High on the continent and the Aleutian Low in the ocean. The climate is maritime and is the coldest in the Okhotsk Sea since it is

an area of accumulation and destruction of drifting ice [14,15]. Ice floes linger here until mid-July and, in some years, until August. Throughout the year, cold dense shelf waters with a temperature about −1.7 °C are preserved around the Shantar Archipelago [16]. Due to contrasting weather pattern, strong northwestern winds and frequent fogs are typical. The average annual air temperature (t) is about −3.5 °C.

In winter, anticyclonic circulation predominates over the continent. Cyclonic activity over the Okhotsk Sea and other Far Eastern seas plays an important role. North-western and northern winds (frequency 70–90%) bring cold dry air masses from the continent. Heavy snowfalls are associated with southern cyclones and cyclones that regenerate (secondary deepening) on the Arctic front. Data from Bolshoy Shantar station (1939–1995) record the snow cover on the islands is 30–50 cm. Winters are relatively mild with mean January temperatures of −15.9 °C and absolute minimums reaching −39.3 °C. In spring, conditions for the development of cyclonic activity over the continent are created and the frequency of western cyclones occurrence increases by 15%. A high-pressure field begins to form over the Far Eastern seas and the Pacific Ocean. In summer, the sea is influenced by the Okhotsk High and cyclone development occurs over the continent. In the warm season from May to July, the introduction of cold air or the passage of cold fronts along with unstable stratification of the atmosphere, leads to the formation of convective squalls and hail during thunder storms. Summer is cool with mean July temperature of +10.5 °C (absolute maximum +30.7 °C) and the frequency of southern cyclones is high and is associated with dangerous weather phenomena such as strong winds, storms, and intense rainfalls. In autumn, there is an increase in cyclone formation in the Yellow and Japan Seas and northeastern China. Typhoons that occur in southern latitudes regenerate into cyclones when passing the Polar front and bring heavy precipitation to the region. The average annual precipitation is 500–522 mm/year and the maximum precipitation occurs in the second half of summer and early autumn [13].

The highest wind speeds are observed in winter and are associated with large pressure gradients in the coastal zone. The average wind speed in November–December is 4.9 m/s, but wind speeds can reach 30 m/s (probability of once per year) to 44 m/s (probability once every 20 years) [13]. The largest number of storms is associated with the emergence of cyclones entering the Okhotsk Sea along sea tracks [17]. From the 1950s, periods of decreased or increased storm activity were identified, lasting from 4 to 11 years. The most intense storms in the western part of the sea result from northern and eastern winds. The northern winds are most intense in autumn when speeds can reach 25 m/s, creating waves on the shelf up to 5 m. In summer, the frequency of storms is 2% [17]. In winter and spring, stable ice coverage prevents the development of storms around the Shantar Islands.

Extreme storms are usually associated with cyclones at 950–980 hPa level [17] and are the most important storms for the formation of marine bioaerosols. In the warm season, such cyclones come from the East China Sea, Yellow Sea and the Pacific Ocean; in the cold season, cyclones also include those that originate over the Japan Sea and the adjacent continental territories. For big waves to develop in a short time (within 6 hours), the wind speeds must be at least 35–40 m/s and the acceleration distance must be 100 km. Typhoons are the most dangerous for the western and southern parts of the Okhotsk Sea and also have a storm effect. Approximately one to four typhoons enter the Okhotsk Sea region per year [17]. Although continental cyclones rarely cause severe storms in the Okhotsk Sea, there are reports of extreme storms associated with the release of continental cyclones [17].

Bolshoy Shantar Island, the largest in the Shantar Archipelago, has a low-mountainous relief with maximum elevation of 701 m. Lowlands are confined to the river's lower reaches and the coast. Peatlands (total area up to 30 km^2) are located in river valleys, within flat watersheds and near lakes. The islands are located in a tectonically stable region [18] and there are no high marine terraces [19]. The inshore zone is steep, except in Yakshin Bay. Abrasion and abrasion-denudation shores prevail and there are many reefs. Irregular semi-diurnal tides (2.7–4.9 m) cause strong currents up to 30–50 cm/s [15]. The interaction of strong currents with the bottom along with the varied configuration of the coastline

leads to the formation of jet currents and eddies (from 4 to 40 km) that affect melt, sea water mixing, and plankton distribution [16,20]. Near the capes, overfalls and breakers on reefs occur, which can also play a role in bioaerosol emission. Water structure in the shallow bays forms under the influence of low-salinity river plumes and vigorous tidal mixing [20].

Three altitudinal vegetation belts are well pronounced on Bolshoy Shantar Island [21]. Spruce (*Picea ajanensis*) and larch forests (*Larix cajanderi*), as well as mixed stone birch (*Betula ermanii*)-spruce and spruce-larch forests are widespread up to 300–400 m. Communities with species typical for nemoral forests occur locally and are confined to river valleys. Forests with dwarf pine (*Pinus pumila*) and alder (*Duschekia fruticosae*, *D. kamtschatica*) occupy steep slopes; small-leaved forests with *B. platyphylla*, and *Populus tremula* are found on the southern slopes. Communities of dwarf pine with *B. middendorfii*, *B. exilis*, *Ledum decumbens* and others occur above 300–400 m. The belt of shrub-lichen vegetation occupies the mountain tops. There are meadows on the marine shores and near river mouths. The island flora is similar to the neighboring parts of the continent and there are no signs of endemism [21].

3. Materials and Methods

The study location is a blanket peat bog in the northern part of Bolshoy Shantar Island. An oligotrophic grass-sphagnum bog is located on the flattened watershed of the Tundrovaya River (55°06′59.1″ N, 137°49′43″ E, height 85 m, 1.5 km from the marine coast) (Figure 1). Peat accumulation began in the Younger Dryas and continued through the Holocene [22]. The peat contains marine diatoms that could have been carried onto land during periods of high storm activity associated with the passage of deep cyclones. The pollen spectra, including those from the surface layer of peat, contain a large amount of pollen from fir, pine, and broad-leaved trees that do not currently grow on the Shantar Islands [21]. Further analysis of these pollen distributions can serve as an indicator of the airflow transport from the continent during the growing season.

The peat was drilled using a Russian peat borer TBG-1. The depth of the sampled section was 390 cm. The sampling interval was 5 cm without gaps; 2 samples were taken below 380 cm with a step of 2.5 cm, and 1 sample from the underlying clay. Botanical, diatom, and pollen analyzes were previously carried out to reconstruct environmental development [22]. Radiocarbon dating of peat samples was performed at the Institute of Monitoring of Climatic and Ecological Systems in the Siberian Branch of the Russian Academy of Sciences. We used an age-depth model (Figure 2) constructed using the Bacon 2.2 package [23]. The temporal resolution of the reconstructions is 360 years, after 9640 cal yr BP 180–200 years, after 4800 cal yr BP 130–134 years, after 2695 cal yr BP 120–125 years, and the last 710 years BP 70–72 years. The peat core temporal resolution is insufficient to identify seasonal fluctuations. We, therefore, estimate seasonal variability during the Holocene based on the typical seasonality of cyclone activity in the 20–21th centuries, as well as from characteristic types of continental and marine aerosol transported to the Shantar Islands from the northern Okhotsk Sea shelf and adjacent land areas.

An additional study of marine diatoms in freshwater assemblages formed in situ was carried out. Marine diatom species could not be redeposited from ancient marine sediments since they are absent above sea level. Marine diatoms are allochthonous and were introduced into the peat bog from the sea; therefore, we consider them to be a sign of the presence of material transferred to land with marine bioaerosols. Sample processing for the diatom analysis was performed following standard procedures [24,25]. The samples were heated to 100°C with 30% hydrogen peroxide (H_2O_2). To calculate the diatom concentration in sediments, 0.2 ml of the suspension was pipetted onto a clean coverslip and the water was evaporated at room temperature. When the coverslips were dry, they were mounted in resin with a refractive index of 1.67–1.68. The diatom samples were then mounted on permanent slides and identified under a microscope (Axioscop) at 1000x magnification and species were identified [26–28]. The entire field (18 mm × 18 mm) of the preparation was examined and measurements were taken of each specimen encountered. Marine and

brackish-water diatoms were counted per 1 g of air-dried sediment and the concentration of residues of various sizes was categorized: up to 10 µm, 10–20 µm and more than 20 µm.
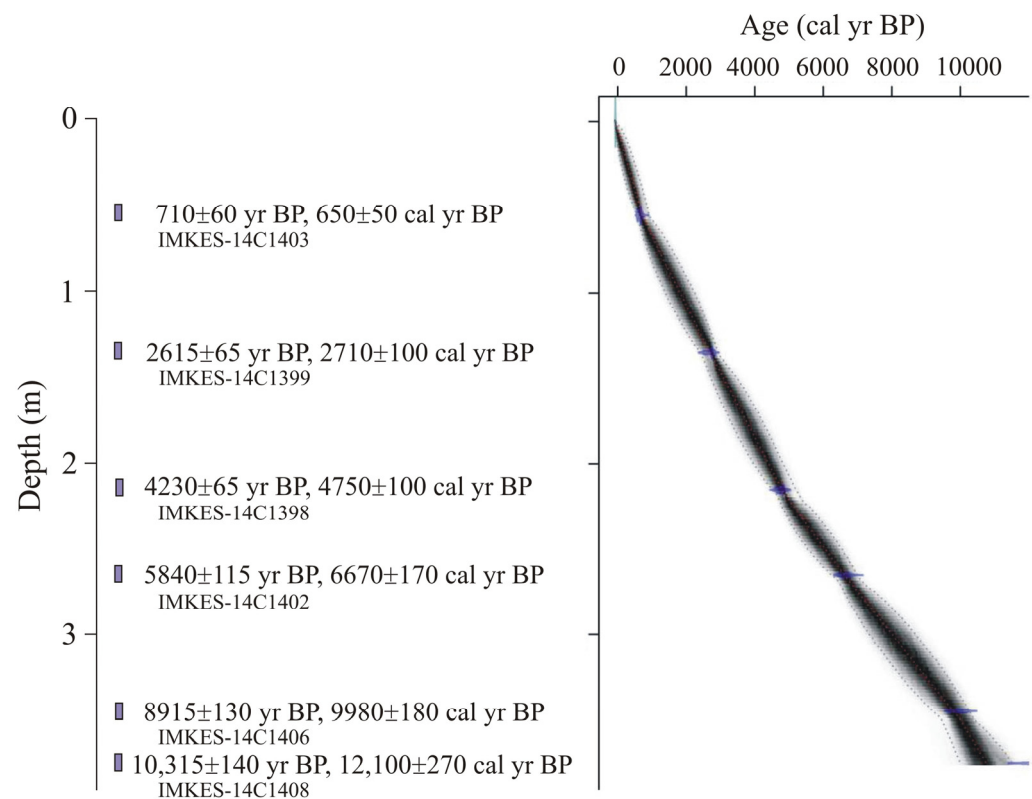
Figure 2. Age-depth relationship for the peat bog section 12716 from Bolshoy Shantar Island, plotted using Bacon [23] with 95% confidence limits.

The samples for pollen analyses were treated using the heavy liquid (2.2 g·cm^{-3}) density separation method [29]. The relative abundances of tree and shrub pollen (arboreal pollen; AP), dwarf shrub and herb pollen (non-arboreal pollen; NAP) and spores were estimated. The proportion of allochthonous AP was calculated from the total amount of AP. The subfossil pollen spectra of modern silt from the Bolotny Creek (Tundrovaya River tributary) and the Argulad River were also studied [22].

The composition of the pollen from plants not growing on the island was also analyzed. In the surface layer of peat, the amount of *Abies* pollen reached 5.4% and, in subfossil pollen spectra was up to 10%. The nearest stands of *Abies nephrolepis* are found on the mainland coast 165 km from the sampled location [30]. The transfer of *Abies sachalinensis* pollen by easterly winds from Northern Sakhalin (distance of more than 330 km) is also possible. Taxa *Pinus* s/g *Diploxylon* most likely belongs to *Pinus sylvestris*. On the mainland *Pinus sylvestris* grows on the coast in the Ayan region, 140 km north from the Bolshoy Shantar Island. From the west, the area with the closest *Pinus* species is located 190 km away, and from the south approximately 230 km away [30]. These taxa (*Abies* and *Pinus* s/g *Diploxylon*) in the study location can be indicators of continental cyclone activity.

The pollen of broad-leaved plants (*Quercus*, *Corylus*, *Carpinus*), representatives of forest vegetation of the East Asian floristic area [31], were found in modern fluvial silts. The northern border of the *Quercus mongolica* range is located 230 km from the study location [32]. Refugia of shrubby oak groves located among dwarf pine are preserved on the coast of Nikolay Bay, 140 km from the study location. The northern border of the range of the hornbeam *Carpinus cordata* is located in South Primorye, 1200–1300 km from Bolshoy Shantar Island. The closest habitat of hazel *Corylus mandshurica* is in the Lower Amur valley, 300 km from the study site [33]. The modern northern border of the range of the nut *Juglans*

mandshurica is 680 km, and the elm *Ulmus* japonica is 240 km from the study location [32,34]. The pollen of oak, hazel, walnut, and elm indicate the activity of continental cyclones coming from the southwest, while hornbeam indicates southern cyclones. The position of the northern boundaries of the ranges of broadleaf trees in the Holocene optimum is known [35–37].

Among the plants that grow on the Shantar islands, dwarf pine (*Pinus* s/g *Haploxylon* pollen) is informative for understanding winter cyclone activity [22] since stable and deep snow cover is required [38,39]. Snowfalls are associated with the passage of cyclones arriving in the cold season from the south [13]. The winter season is characterized by cyclones that originate over the Japan Sea [17].

4. Results

4.1. Diatoms

Fragments and whole valves of 55 taxa of marine and brackish-water diatoms, including extinct species, were found in the peat bog (Figure 3, Table S1). Forty-four taxa were identified to the species level. Thirteen oceanic and neritic species were found, including fossil species (*Thalassiosira insigna*, *Actinocyclus ingens*, *A. ochotensis* var. *fossilis*, *Eupyxidicula zabelinae*). These species are planktonic and inhabit the upper photic layer. Most of the species are cold-water. The vegetation of the arctoboreal *Thalassiosira gravida* occurs near the sea ice edge [40]. Northboreal *Actinocyclus curvatulus*, *Actinocyclus ochotensis* and arctoboreal *Porosira glacialis* inhabit the north of the subarctic front, including the Okhotsk and Bering Seas and the seas of the Eastern Arctic [28,41,42]. The cosmopolite *Thalassionema nitzschioides* is widespread in the region of the subarctic front, the North Pacific Ocean, and the Eastern Arctic [28,41]. This species is abundant (up to 30%) in the bottom sediments of the southwestern part of the Okhotsk Sea, which is possibly related to the influence of the warm waters of the Kuroshio Current [42]. *Paralia sulcata* is characteristic of deposits of the last maximum cooling and is an indicator of freshening (up to 25‰) [41]. Regarding the Okhotsk Sea, it is considered as an indicator species for periods of active ice melting and surface water freshening [43].
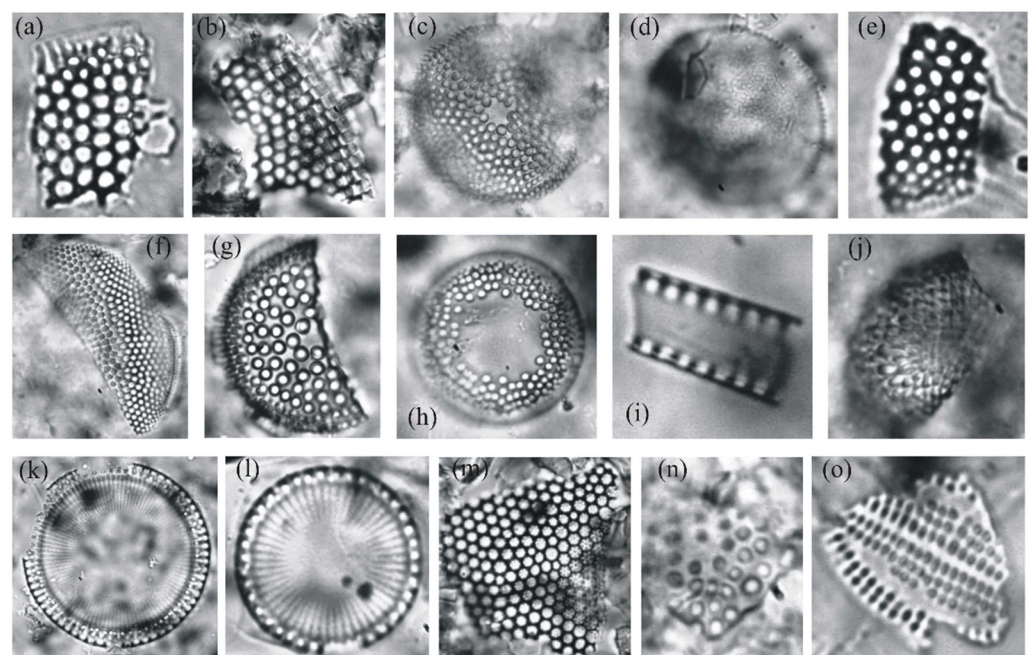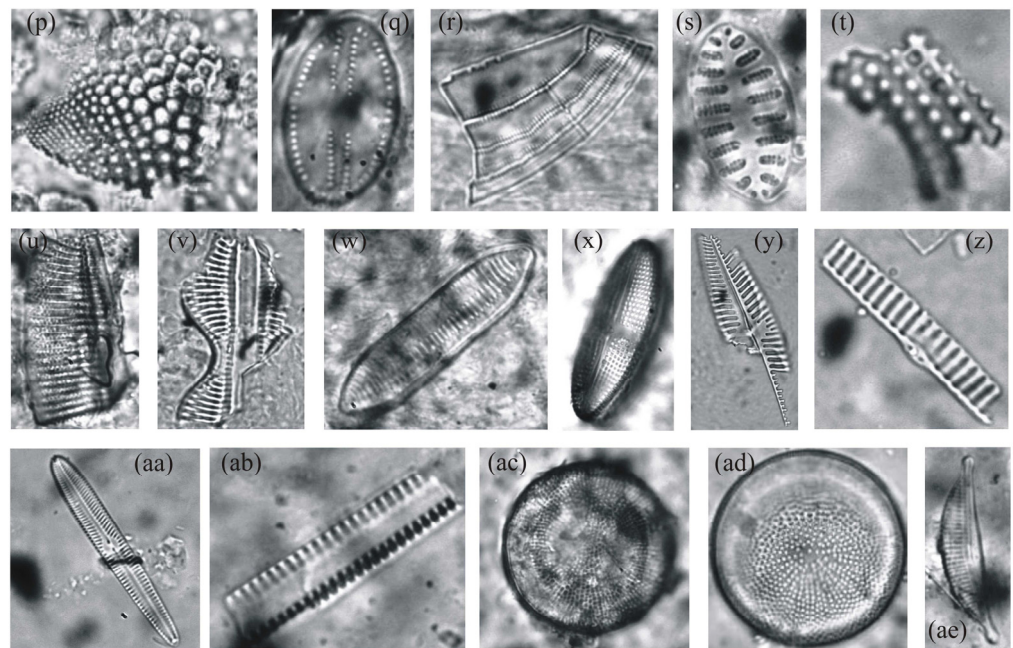

Figure 3. *Cont.*

Figure 3. Photo of marine diatoms from the peat bog of Bolshoy Shantar Island. Oceanic and neritic species: (**a**) *Coscinodiscus* sp. 10 μm × 15 μm; (**b**) *Thalassiosira* sp. 15 μm × 19 μm; (**c**) *Actinocyclus ochotensis* 24 μm × 24 μm; (**d**) *Porosira glacialis* 25 μm × 25 μm; (**e**) *Thalassiosira gravida* 9 μm × 18 μm; (**f**) *Actinocyclus curvatulus* 15 μm × 40 μm; (**g**) *Actinocyclus ingens* 26 μm × 13 μm; (**h**) *Thalassiosira insigna* 25 μm × 25 μm; (**i**) *Thalassionema nitzschioides* 4 μm × 8 μm; (**j**) *Eupyxidicula zabelinae* 13 μm × 20 μm; (**k**) *Paralia sulcata* var. *biseriata* 5 μm × 45 μm; (**l**) *Paralia sulcata* 18 μm × 18 μm; (**m**) *Coscinodiscus asteromphalus* 18 μm × 15 μm; (**n**) *Actinocyclus ochotensis* var. *fossilis* 8 × 6 μm; Sublittoral species: (**o**) *Cocconeis californica* 8 μm × 12 μm; (**p**) *Trigonium arcticum* 19 μm × 14 μm; (**q**) *Cocconeis infirmata* 22 μm × 13 μm; (**r**) C. aff. *pellucida* 34 μm × 18 μm; (**s**) *C. costata* 20 μm × 11 μm; (**t**) – *C. scutellum* 5 μm × 9 μm; (**u**) *Diploneis smithii* 30 μm × 17 μm; (**v**) *D. interrupta* 30 μm × 19 μm; (**w**) *Tryblionella levidensis* 43 μm × 13 μm; (**x**) *Achnanthes brevipes* 43 μm × 17 μm; (**y**) *Navicula distans* 22 μm × 77 μm; (**z**) – *N. directa* 3 μm × 22 μm; (**aa**) *Pseudogomphonema kamtchaticum* 13 μm × 6 μm; (**ab**) *Tabularia tabulata* 3 μm × 15 μm; (**ac**) *Thalassiosira bramaputrae* 31 μm × 31 μm; (**ad**) *Actinocyclus octonarius* 16 μm × 16 μm; (**ae**) *Halamphora coffeiformis* 25 μm × 12 μm.

Sublittoral species include the planktonic-benthic *Actinocyclus octonarius*, the planktonic *Thalassiosira bramaputrae*, and 29 benthic forms. Among them, sea-ice epiphytes *Pseudogomphonema kamtchaticum* that attach to ice [44], and *Trigonium arcticum* were found under ice in surface sediments of Prydz Bay in East Antarctica [45]. The distribution of marine and brackish-water diatoms along the peat bog section is extremely uneven. Fifteen intervals where marine species of different ecology were encountered and that correspond to the phases of active removal and deposition of bioaerosols on the island were identified (Figure 4).

Depth 365–370 cm (11770–11410 cal yr BP, phase 1): A large number of marine and brackish-water species (>6 × 10³ valves/g) were found, belonging to 14 taxa. Fragments of valves of sublittoral species up to 10 μm in size prevail, while *Cocconeis scutellum* and *Actinocyclus octonarius* dominate. The ice epiphyte *Pseudogomphonema kamtchaticum* that inhabits estuaries, limans, lagoons [46] and *Melosira moniliformis*, *Tabularia tabulata*, *Ctehophora pulchella* were present. Fragments of oceanic and neritic species were found, and there are many cosmopolite *Thalassionema nitzschioides*.
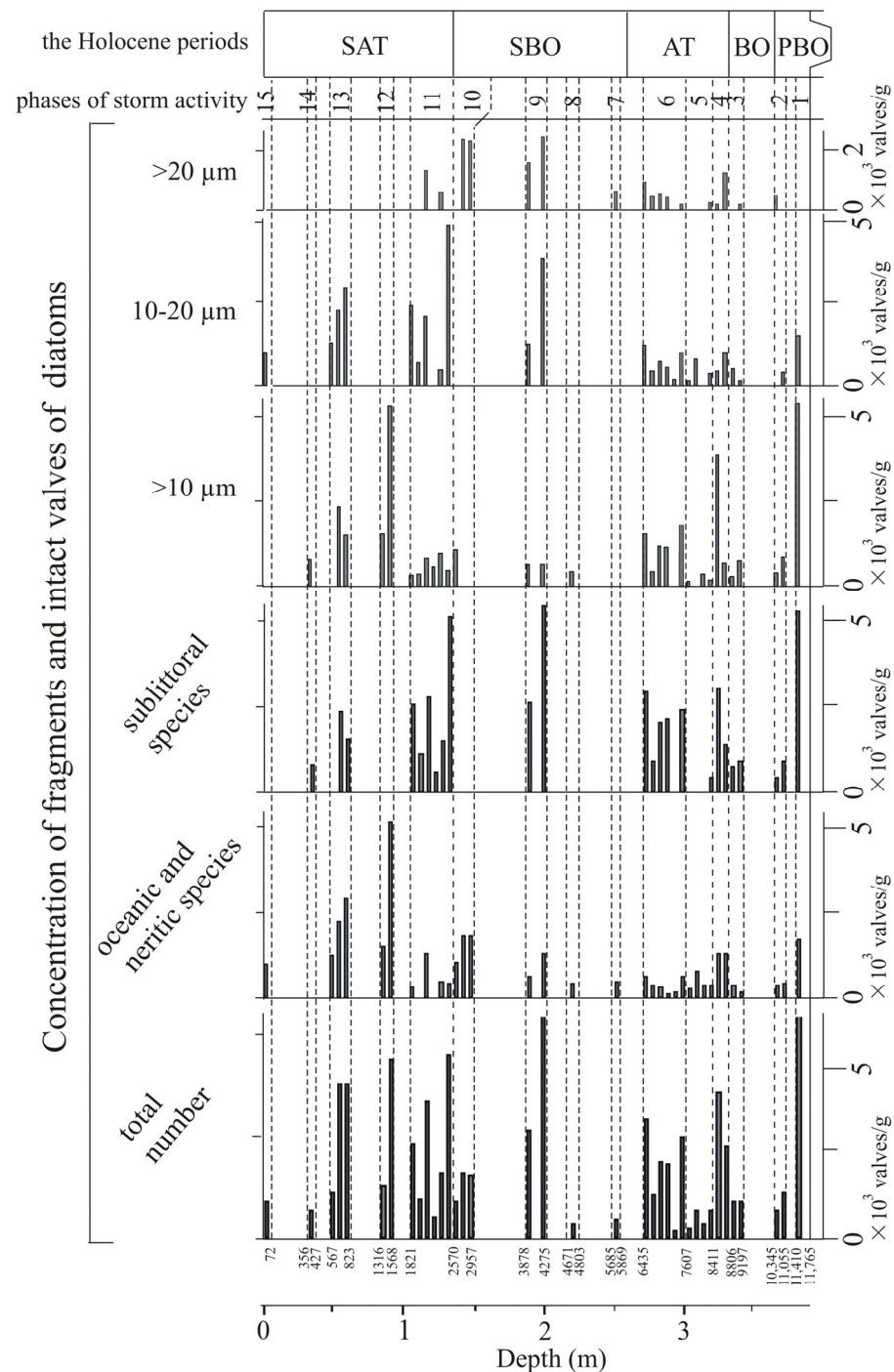
Figure 4. Concentration of allochthonous marine diatoms for the peat bog of Bolshoy Shantar Island that made it possible to distinguish 15 phases of high storm activity in the Holocene. This includes total number, species of different ecology and valves of different sizes.

Depth 350–360 cm (11060–10350 cal yr BP, phase 2): A small number of valves and fragments were found. The proportion of sublittoral and deep-sea species is approximately equal. Among the sublittoral species, *Trigonium arcticum* and *Nitzschia sigma* appeared, which are euryhaline and widespread in estuaries, lagoons, and limans. The deep-water species are represented by fragments of *Thalassiosira* sp. Large valve fragments (>20 μm) appeared.

Depth 320–330 cm (9200–8810 cal yr BP, phase 3): Fragments of valves of sublittoral species predominate. For the deep-sea species, whole valves of cold-water *Actinocyclus ochotensis* and fragments of *Thalassiosira* sp. were found. Fragments of fossil *Thalassiosira*

insigna were found, which went extinct in the Late Pliocene [47], along with zonal species *Actinocyclus ochotensis* var. *fossilis* that became extinct in the Middle Pleistocene [48].

Depth 310–320 cm (8810–8410 cal yr BP, phase 4): The concentration of fragments of marine and brackish-water species sharply increases. Fragments of diatoms more than 20 microns in size were found, including whole valves of *Porosira glacialis*, *Paralia sulcata* var. *biseriata* and fossil *Thalassiosira insigna*, *Actinocyclus ingens*, along with small fragments of *Thalassionema nitzschioides*. The content of large forms and fragments reaches more than 1.3×10^3 valves/g.

Depth 290–310 cm (8410–7610 cal yr BP, phase 5): The valve concentration decreases to 0.82×10^3 valves/g. Many fragments and whole valves 10–20 μm in size were found. *Cocconeis scutellum*, *Paralia sulcata* var. *biseriata*, *Navicula distans*, typical for bays, and the brackish-freshwater *Thalassiosira bramaputrae* appear. In more recent years (8200–7610 cal yr BP), only fragments of neritic and oceanic species are found.

Depth 260–290cm (7610–6440 cal yr BP, phase 6): The concentration of marine diatoms increases to 3.56×10^3 valves/g. Fragments and whole valves of 26 taxa were found, including 1 valve of fossil *Eupyxidicula zabelinae* that went extinct in the Early Pleistocene [48]. Fragments of sublittoral species predominate, but their composition varies along the section. In the depth from 285–290 cm (7610–7410 cal yr BP) *Cocconeis scutellum* and *Actinocyclus octonarius* dominate. There are very few marine diatoms from 280–285 cm (7410–7210 cal yr BP). From 260–280 cm (7210–6440 cal yr BP) fragments of species typical of freshened coastal waters and river mouths were also found: *Thalassiosira bramaputrae*, *Ctenophora pulchella*, *Tabularia tabulata* and brackish-water *Melosira moniliformis*, *M. lineata* that inhabit marine sediments from depth of 0.5 m to 10 m [49]. The concentration of neritic and oceanic diatoms fragments ranges from 0.12 to 0.8×10^3 valves/g. Valves fragments of species of the genera *Thalassiosira* and *Coscinodiscus* are found most. Fragments up to 10 microns in size predominate, but a gradual increase in the number of large fragments was observed. The highest content of large valves and fragments were found at the top of the layer depth (at 260–265 cm, 6620–6440 cal yr BP).

Depth 240–245 cm (5870–5690 cal yr BP, phase 7): Only fragments of the brackish-water benthic *Hyalodiscus sphaerophorus* were found.

Depth 210–215 cm (4800–4670 cal yr BP, phase 8): Fragments of *Paralia sulcata* (0.4×10^3 valves/g) were found.

Depth 180–195 cm (4280–3880 cal yr BP, phase 9): A large number of marine diatoms were found. Large fragments and whole valves (10–20 μm and $\geq$20 μm) of sublittoral species prevail. The highest concentration (6.7×10^3 valves/g) was noted in the depth 190–195 cm (4280–4140 cal yr BP). The dominant species is the marine epiphyte *Cocconeis costata* that lives at depths of 0.3–10 m [49]; all valves are intact. Whole valves of *Tryblionella levidensis* and *C. scutellum*, and fragments of *Tabularia tabulata*, typical of lagoons and lagoon lakes, were also found. Oceanic and neritic diatoms are represented by fragments of *Thalassiosira* sp., their concentration is $\geq 1.3 \times 10^3$ valves/g. From 180–185 cm (4010–3880 cal yr BP) *Pinnunavis yarrensis*, *Diploneis smithii*, *Grammatophora* sp. appeared.

Depth 130–145 cm (2960–2570 cal yr BP, phase 10): In the lower part of the segment (depth 135–145 cm, 2960–2700 cal yr BP) only large fragments ($\geq$20 μm) of oceanic-neritic species of the genus *Thalassiosira* were found. In the higher part of the segment, (depth 130–135 m, 2700–2570 cal yr BP), small fragments of oceanic species of the genus *Coscinodiscus* were found.

Depth 100–130 cm (2570–1820 cal yr BP, phase 11): Marine and brackish-water diatoms common in inshore waters dominate. Fragments and whole valves of 21 taxa were found. The highest concentration (up to 5.5×10^3 valves/g) was noted from 125–130 cm (2570–2450 cal yr BP) and 110–115 cm (2200–2070 cal yr BP). Entire valves of *Cocconeis costata* dominated. There are large fragments (10–20 microns and $\geq$20 μm) of *Halamphora coffeiformis* and *Diploneis interrupta*, typical for bays, as well as inhabitants of the northern seas *Navicula distans*, *Cocconeis californica*, *C. infirmata*. Sublittoral warm-water *Cocconeis* aff. *pellucida* and brackish-freshwater *Thalassiosira bramaputrae* occur. A high concentration

$(1.4 \times 10^3$ valves/g) of fragments of neritic and oceanic diatoms (*Thalassiosira*, *Coscinodiscus* and *Thalassionema nitzschioides*) was noted from 110–115 cm (2200–2070 cal yr BP).

Depth 80–90 cm (1570–1320 cal yr BP, phase 12): There is a high concentration of marine species (up to 5.4×10^3 valves/g). Only small fragments (up to 10 μm) of oceanic and neritic species are present.

Depth 45–60 cm (820–570 cal yr BP, phase 13): The lower part contains fragments of neritic and oceanic *Thalassionema nitzschioides*, *Coscinodiscus asteromphalus*, *Coscinodiscus* sp. and inhabitants of bays *Cocconeis costata*, *C. scutellum*, *Navicula directa*. Valves and fragments are large (up to 20 μm). The upper part (640–570 cal yr BP) contains only fragments of *Coscinodiscus* sp.

Depth 30–35 cm (430–360 cal yr BP, phase 14): The concentration of marine species is low. Whole valves of *Cocconeis californica* was found.

Depth 0–5 cm (last 70 years, phase 15): Fragments (up to 20 μm in size) of the arctoboreal *Thalassiosira gravida* were found.

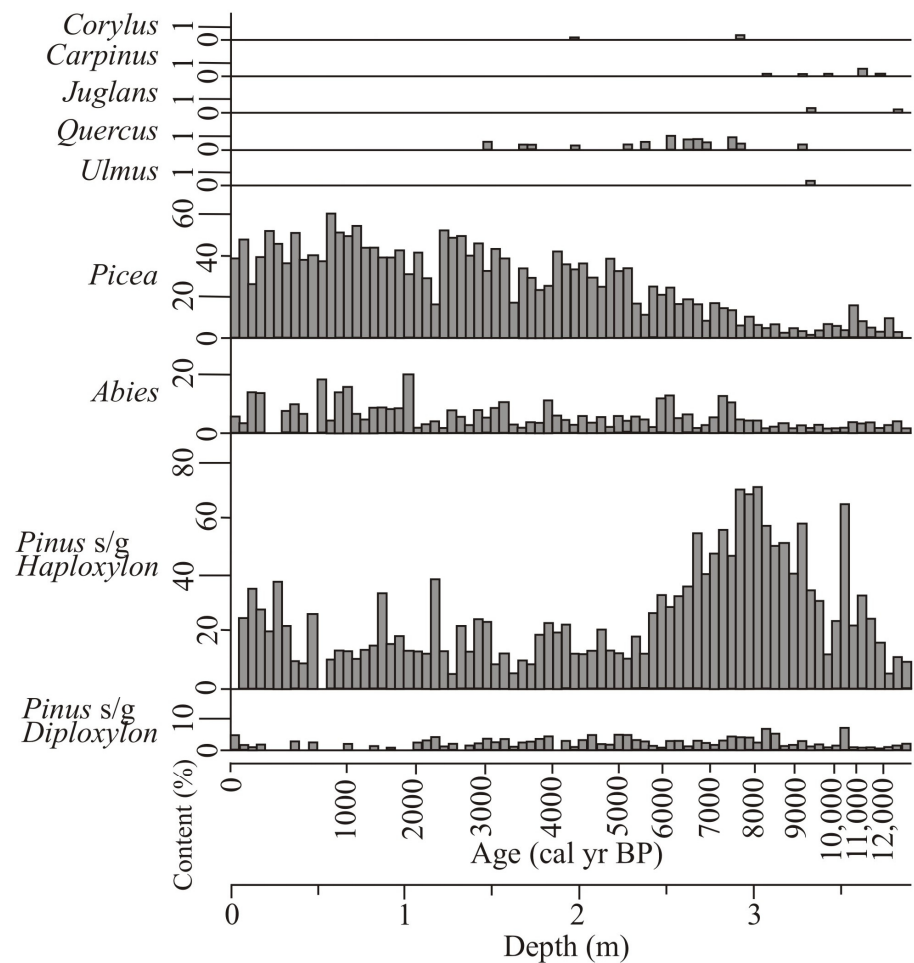*4.2. Pollen*

The distribution of allochthonous pollen in the section is uneven (Figure 5). The main source of allochthonous pollen was from the mainland via wind transport in the form of bioaerosols. In wind-blown pollen in the sediments, the pollen of the fir (*Abies*) is the most common. A small amount of this pollen (up to 3.9%) is present in the clay underlying the peat bog and the peat from the base of the section that formed in the Younger Dryas and at the boundary of the Late Pleistocene–Holocene. Two peaks of pollen were recorded at 12480–12120 cal yr BP and 11400–10350 cal yr BP. In peat formed at the beginning of the Holocene (10350–9400 cal yr BP), only single *Abies* pollen were found (<1%). At a depth of 335–285 cm, the pollen content is low (<4.4%). More intense pollen input was recorded at a depth of 285 cm (from 7410 cal yr BP), where peaks up to 13.5% were noted. The highest proportions (depth 275–285, 240–250, 180–185, 155–160 cm) correspond to the ages 7410–7010, 6060–5690, 4010–3880, and 3360–3220 cal yr BP. Low contents are recorded in peat formed about 6810–6440, 5690–5500, 4800–4670, 4280–4140, 3880–3360, 2450–1950 cal yr PB (depth 260–270, 235–240, 210–215, 190–195, 160–180, 105–125 cm, respectively). An increase in *Abies* pollen (up to 20%) was observed in peat formed during 1950–640 cal yr BP (depth 50–105 cm). The peaks (depth 100–105, 60–70, 50–55 cm) correspond to 1950–1820, 1070–820, and 710–640 cal yr BP. During the Little Ice Age, there was a sharp increase in the pollen content, ranging from 0 to 13.9%. The peaks were recorded in peat (depth 35–40, 10–20 cm), formed during 500–430 cal yr BP, and from 220 cal yr BP to the end of the 19th century.

The pollen content of *Pinus* s/g *Diploxylon* varied from single grains to 6.9%. For most of the sediment core, peaks in pine pollen coincided with peaks of *Abies* pollen. The exception was at depths of 240–250 cm (6060–5690 cal yr BP), where the reverse movement is noted and the proportion of pine pollen was <1%. In the upper part in the core (last 1950 cal yr BP), the amount of pine pollen decreased (less than 2.5%) until it disappeared. In the surface layer of peat, the proportion of pine pollen was 4.5%, which reflects the transfer by bioaerosols, corresponding to modern air circulation.

In the Younger Dryas and Early Holocene, spruce pollen (*Picea*) was also transported as bioaerosols. Spruce forests appeared in the region starting at 7610 cal yr BP [22]. Until that time, the peaks of *Picea* pollen coincided with the peaks of *Abies*, corresponding to the pollen transfer of these taxa from the zone of dark coniferous forests. The first peak is noted from 12,480–12,120 cal yr BP and the second from 11,060–10,700 cal yr BP. The total pollen content from broad-leaved species was insignificant (up to 1%). Single grains of *Carpinus* and *Juglans* were found in peat formed in the Younger Dryas; *Carpinus* was found in peat formed at the beginning of the Holocene. In 9400–9000 cal yr BP, pollen of *Quercus* and *Ulmus* appeared along with *Carpinus* and *Juglans*. Oak pollen became more common from 7810 cal yr BP and *Corylus* pollen appeared sporadically. Periodically, there were intervals where broad-leaved pollen was absent, and broad-leaved pollen was absent

in the upper part of the section. Modern fluvial silts contained single pollen of *Quercus*, *Corylus*, *Carpinus*.

Figure 5. Distribution of allochtonous pollen (*Pinus* s/g *Diploxylon*, *Abies*, *Ulmus*, *Quercus*, *Juglans*, *Carpinus*, *Corylus*) and two taxon (*Pinus* s/g *Haploxylon* and *Picea*) of plants that grow on Bolshoy Shantar Island in the peat bog. The distribution of allochthonous pollen indicate continental cyclone activity in the Shantar region in late spring and early summer. *Pinus* s/g *Haploxylon* is informative for understanding winter cyclone activity. *Picea* pollen was also transported as bioaerosols up to the Middle Holocene, with spruce forests becoming widespread in the Shantar Islands starting in 7610 cal yr BP.

5. Discussion

The finding of marine diatoms and allochthonous pollen that were transferred to the territory of the Shantar Islands, in the form of bioaerosols, make it possible to distinguish periods of increased storm activity and changes in circulation and intense cyclogenesis over the last 12,650 cal yrs. Marine diatoms entering coastal areas with other aerosols from the sea during extreme storms most likely record the passage of marine cyclones. Marine diatoms are indirect indicators of the activation of cyclogenesis; the main period of storm activity in this part of the Okhotsk Sea is associated with typhoons and the emergence of deep cyclones in autumn before coastal waters freeze [17]. Cyclones arriving in the Okhotsk Sea begin in the East China and Japan Seas and east of Japan [50]. Exceptionally strong waves can develop during the passage of secondary cyclones, including cyclones from the continent. An example of this extreme event was a storm from 10–12 November, 1969 that started as a deep cyclone from the continent and joined a depression in the Shantar Islands,

where it deepened to 980 hPa and remained stationary for 1.5 days. Wave heights reached 8–10 m in the western part of the Okhotsk Sea [17].

The emission mechanism of marine bioaerosols during strong storms is associated with the formation and destruction of bubbles. When a bubble with a diameter of 2 mm breaks down, up to 2000 drops are formed and those drops can capture phytoplankton and be carried off by the wind [5]. In the open sea, phytoplankton is captured from the surface layer, where the maximum of diatom production is observed [51,52].

At the beginning of the Holocene, the disappearance of diatom valves and their fragments could also have occurred from the drained shelf. In the Younger Dryas, the sea level was 50–55 m below present, and before the Holocene it was 43–47 m below present [36,53]. The vast shallow water area between the Shantar Islands and the modern mainland constituted a land bridge. The coastline was located 10 km from the northern coast of the Bolshoy Shantar Island. In the Younger Dryas, the climatic conditions were severe and permafrost developed on the drained shelf. In the early Holocene, the transfer of marine diatoms occurred under milder climatic conditions.

Judging by depth, Bolshoy Shantar Island separated from the mainland during the Early-Middle Holocene. The islands separated from the continent and the vast Shantar Sea was formed [22]. Sea level reached its current high and then began to rise 2–3 m above present-day levels of around 7000–6800 cal yr BP. Since that period, the emission of aerosols with marine diatoms into terrestrial regions could only occur during storms.

Pollen is present in atmospheric aerosols throughout the growing season, but high concentrations of pollen from anemophilous plants occur during the period of flowering [54]. Flowering of trees that do not grow on the Shantar Islands, the pollen of which was brought to Bolshoy Shantar Island from bioaerosols, occurs in spring to early summer. The data obtained on the distribution of allochthonous pollen indicate that continental cyclones emerged in the Shantar region in late spring and early summer.

The distribution of allochthonous microfossils made it possible to distinguish 15 phases of high storm activity in the Holocene and regularities of atmospheric circulation at the end of the Pleistocene–Holocene (Figure 6). Cold periods were evident from increases in freshwater arctoboreal diatoms.

5.1. Younger Dryas–Early Holocene

In the Younger Dryas and early Holocene, the peaks of fir and spruce pollen (Figure 6) indicate that the active influx of bioaerosols from the zone of dark coniferous forests were due to cyclones emanating from the southwest. Two peaks in the pollen of these taxa correspond to cold episodes with high wind activity (12,475–12,120 cal yr BP, 11,400–10,345 cal yr BP). The absence of marine aerosols transport to land may have been connected, not only with the large distance of the studied area from the sea, but also explained by the low productivity of diatoms under conditions of a short growing season and stable ice coverage in the Younger Dryas [43].

During this time, there was a land bridge connecting the Shantar Islands to the continent. Shrub communities (birch, alder and dwarf pine) grew in the areas that would be future islands [22]. For this region, there is no exact data on the position of the northern border of dark coniferous forests. In the Gursky peat bog, one of the oldest in the Lower Amur region, the border of the area of dark coniferous forests was south of 50° N [55]. Dark coniferous forests with a predominance of spruce existed at that time in the region of the Bikin River valley (northern Sikhote-Alin mountains) [56]. Pollen was transported at least 500 km. Spruce forests developed in the northwest of Sakhalin Island (Khoe section) [57,58]. It is possible that spruce pollen could be partially transported by southern and southeastern airflows. The transfer of bioaerosols from the south is confirmed by the findings of hornbeam and walnut pollen (*Carpinus*, and *Juglans*). Moreover, the transfer of pollen likely came from the Korean Peninsula (at a distance of 1500–1700 km), since *Carpinus* and *Juglans* appeared in southern Primorye and northeastern China about 9300 cal

yr BP during a period of warming and increasing moisture [59,60]. At present, the cyclones track from the south in late spring and early summer are not typical for the region [13,61].
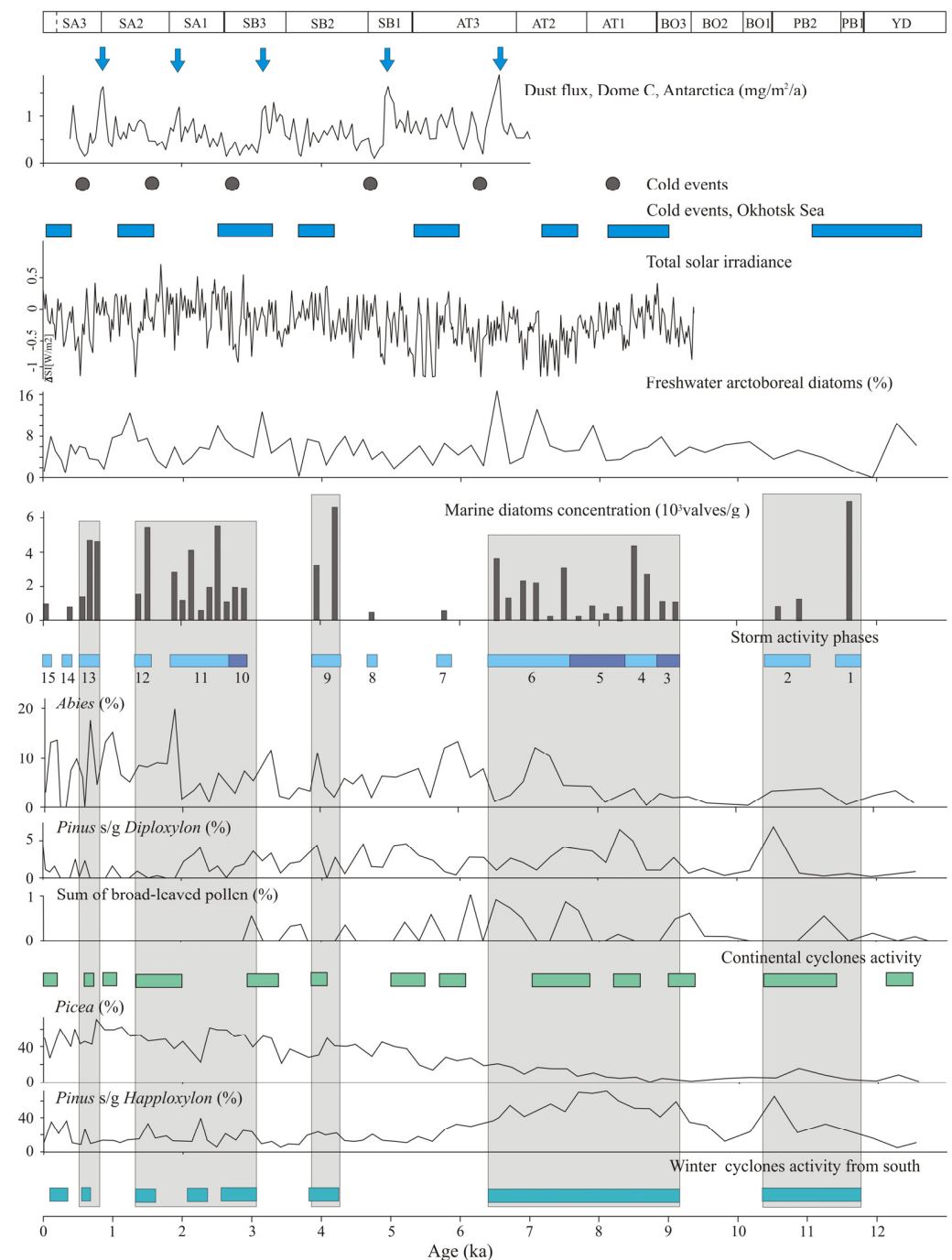
Figure 6. Changes in the concentration of marine diatoms and relative abundance of allochtonous pollen according to an age-depth model for peat bog sections in Late Glacial-Holocene. A time series of dust flux at Dome C, Antarctica, is shown as vertical blue arrows point to wind termini, according to [62]; changes in the solar activity are based on ^{10}Be measurements in the polar ice are given according to [63]; global Holocene cold events, according to [64]; cold events in the Okhotsk Sea, according to [65]; and Holocene subdivision, according to [66]. Gray bars show the periods of intensification of cyclogenesis.

At the end of the Younger Dryas and the early Holocene, three phases (phases 1–3) of increased storm activity (11,770–11,410, 11,060–10,350, 9200–8810 cal yr BP, respectively),

apparently associated with the passage of southern cyclones in cold seasons, were distinguished (Figures 4 and 6). In phase 1, the most active entry of marine diatoms into the northern part of Bolshoy Shantar Island took place. During Deglaciation (15,000–10,000 cal yr BP), the distribution of marine ice expanded into the northern and western parts of the Okhotsk Sea. A strong decrease in ice rafted debris (IRD) indicates an increase in the marine ice coverage in the western part of the sea 12,600–11,100 cal yr BP [43]. Under the intensification of the Siberian High, western and north-western winds prevailed, wherein extensive polynyas formed on the northern continental shelf of the Okhotsk Sea [67]. The presence of epiphytes *Pseudogomphonema kamtchaticum*, *Trigonium arcticum*, inhabiting the ice edge (phases 1–2) in the peat bog section possibly indicates that the emission of bioaerosols could occur from polynyas.

The sea level in the early Holocene was at –30 to –25 m below present [36,68] and the coast was located 4.5 km from the study area. The abundance of fragments of benthic diatoms and the presence of fossil *Tlalassiosira insigna* and *Actinocyclus ingens* that became extinct in the Neogene [47], as well as the Middle Pleistocene zonal species *Actinocyclus ochotensis* var. *fossilis* [48], suggest that most of the marine and brackish-water diatom fragments were transported from the drained shelf. It cannot be ruled out that the fossil species could have been brought with aerosols from Sakhalin Island, where Neogene and Quaternary marine sediments are widespread [69]. The high degree of fragmentation of the diatom valves could be associated with their prolonged stay in subaerial conditions. It cannot be excluded that valves were crushed by sea ice drifting under the influence of storm winds. During periods of extreme storms, diatoms were also transported from the open sea. An increase in diatom productivity in the Early Holocene (11,100–9100 cal yr BP) and an increase in the growing season along with a decrease in ice coverage leads to more intensive supply of marine bioaerosols to the Shantar Islands. An increase in IRD at the beginning of the Holocene indicates an increase in sea ice melting in the summer season [43]. The presence of marine diatoms in peat correlates well with peaks of dwarf pine pollen. It can be assumed that intense storm events occurred during periods of increased intensity of southern cyclones causing extreme snowfalls.

During this period, the transport of pollen from remote southwestern regions (the basin of the lower reaches of the Amur River), where dark coniferous forests have already appeared [55], significantly decreased due to a decrease in the frequency and intensity of continental cyclones of southwestern trajectories in late spring and the beginning of summer. The peak of pine pollen *Pinus* s/g *Diploxylon* confirms that 10,700–10,350 cal yr BP bioaerosols were supplied mainly from the west. The minimum import of fir pollen was recorded at 10,350–9400 cal yr BP. At this time, humidity decreased on the islands and there was slight warming that also occurs in other regions of northeastern Asia [66]. The warm period from 10,500–9000 cal yr BP corresponds to the minimum area of ice cover and the development of polynyas in the northern part of the Sea of Okhotsk [70]. Drought conditions around 9300–8900 cal yr BP in the Lower Amur Region were associated with a decrease in the intensity of the summer monsoon [71]. A cold and dry episode ~9300 cal yr BP occurred in the northwest of Sakhalin Island [58].

The appearance of broadleaf pollen (*Quercus*, *Ulmus*, *Carpinus*, *Juglans*) in 9401–9000 cal yr BP indicates an increase in the activity of southwestern and southern cyclones under conditions of cooling at the Early-Middle Holocene boundary [66]. By this time, oak, elm, and walnut appeared in the Lower Amur Region [55]. The distribution of broad-leaved plants was also recorded in northwestern Sakhalin (9300 cal yr BP), in Primorye (~9490–9280 cal yr BP) and northeastern China (~9300–9200 cal yr BP) [59,60,66]. Pollen transport could also occur with southern cyclones.

5.2. Middle Holocene

There are four phases (phases 4–7) of storm activity. In 8810–8410 cal yr BP (phase 4), during strong storms, diatoms were transported, not only from drained shelf, but also from the open sea. Bioaerosols include both fragments and whole valves. At this time, there was

a rapid rise in sea level and flooding of the shelf. The bioaerosols contained species typical for near-ice groups (*Porosira glacialis*, *Thalassiosira gravida*) and *Paralia sulcata* var. *biseriata* became common. The peak of IRD at 9100–8000 cal yr BP indicates an active melting of sea ice [43].

Frequency of extreme storms appeared to decrease in 8410–7610 cal yr BP (phase 5). The maximum content of dwarf pine pollen in the core indicates activation of southern cyclones in the winter season at this time. Marine bioaerosols came mainly from the open sea and in 8200–7610 cal yr BP, fragments of valves of neritic and oceanic diatoms no longer occurred. The removal of bioaerosols possibly took place in winter when water near Shantar Islands was frozen. In 8200 cal yr BP, there was a global cold event that manifested itself in the northern Hemisphere [63,64]. Cooling in East Asia was accompanied by a decrease in moisture associated with a weakening East Asian monsoon from ~8400–8100 cal yr BP that occurred in northeastern China [72], the North-Eastern Asian monsoon in Priamurye [71] and the northwestern Sakhalin [58].

A long period of storm activity was observed from 7610–6440 cal yr BP (phase 6). It partially coincided with the Holocene thermal maximum from 7000–5000 cal yr BP in the Okhotsk Sea [70]. The subperiod 7240–6500 yr BP was especially warm [73]. In the warmer conditions of the Middle Holocene, the sea ice coverage in the western part of the sea greatly decreased [43]. The duration of the growing season and the productivity of diatoms increased. This is the last phase when near-ice diatom groups were found in marine aerosols. *Paralia sulcata*, an indicator of fresh water and ice melting under conditions of progressive warming, began to occur more frequently. The frequency of severe storms in the Shantar region increased significantly. The sea level at that time had already reached the modern position or slightly exceeded it by 2 to 3 m [36,73]. The main transfer of diatoms occurred from shallow waters and the surf zone. Frequency of severe storms decreased from 7410–7210 cal yr BP. During 7210–6440 cal yr BP, in addition to the transfer from the sea, there was an introduction of brackish-water species from the lagoon that formed at the peak of the transgression on the place of the present-day Bolshoye Lake, 10 km southeast from the study area. The length of the lagoon was 13–15 km inland. Brackish-water species could also be carried out from zones of plumes with low salinity, typical of shallow sea near the islands [20]. The high content of large valves and their fragments also highlight nearby transfer (6620–6440 cal yr BP). Fossil *Eupyxidicula zabelinae*, extinct in the Early Pleistocene [48], could have been transferred from Sakhalin Island.

Storm activity phases 3–6 corresponded to the long period of high activity of southern cyclones in the autumn-winter seasons. The high content of dwarf pine pollen shows indirect evidence of increased cyclogenesis in the cold season.

At the end of the Middle Holocene, storm activity decreased. Rare strong storms occurred from 5870–5690 cal yr BP (phase 7). Finds of brackish-water benthic *Hyalodiscus sphaerophorus* likely indicate transfer from the lagoon. Increase in moisture on the Bolshoy Shantar Island indicates an increase in summer cyclogenesis from 6060 to 5690 cal yr BP. On northern Sakhalin an episode of high moisture content, possibly the maximum for the Middle Holocene, was identified and had temperatures similar to the present [74]. In the south of Okhotsk Sea, there was a warm subperiod from 5900 to 4550 cal yr BP when the warm Kuroshio Current was more intense [73].

Removal of pine pollen from the continent intensified from 8610 to 8200 cal yr BP, and the number of continental cyclones with western and northwestern tracks increased. A sharp increase in the supply of fir pollen in the Middle Holocene was associated with a shift in the boundaries of dark-coniferous forests. Spruce forests became widespread in the Shantar Islands starting in 7610 cal yr BP. We believe that there was no fir on Bolshoy Shantar Island, because the pollen content does not exceed its proportion in subfossil pollen spectra. The most intense entrance of fir pollen to the islands occurred at 7410–7010 and 6060–5690 cal yr BP, which is evidence of an increase in the frequency of western and southwestern cyclones. The proportion of pine pollen in bioaerosols decreased during this time.

The oak and hazel pollen began to occur more frequently in bioaerosols from 7810 cal yr BP and is also associated with the displacement of the northern boundary of coniferous-broadleaved forests on the continent near the Amur River mouth (120–150 km north of its present position) [37,55]. In general, the composition of allochthonous pollen reflects the activation of continental cyclones from the south-southwest. In the Holocene optimum, the hornbeam range boundary along the Japan Sea coast shifted northward up to 700 km from its present position [35,36]. No hornbeam pollen was found in the Middle Holocene section of the peat bog on Bolshoy Shantar Island, indicating that there was no transfer of pollen from the extreme south with southern cyclones in late spring and early summer.

5.3. Late Holocene

Extreme storms occurred from 4800–4670 cal yr BP (phase 8). The 4800–4600 cal yr BP phase is identified as one of the global cold events of the Holocene [64]. The removal of only the neritic *Paralia sulcata* indicates the emission of aerosols during storms in the open sea. The ice coverage in the nearby sea was probably established at an earlier time and prevented the development of strong storms in shallow water in the autumn-winter season. Cooling on the Shantar Islands was accompanied by drying [22] that was also observed in the Lower Amur region of 5200–4700 cal yr BP [71] and northern Japan [73]. This indicates a decrease in the activity of cyclogenesis in the warm season when the main atmospheric precipitation falls. The number of allochthonous lacustrine-rheophilic diatoms in the studied section on the Bolshoy Shantar Island confirms that recurrence of floods increased from 4670 to 4540 cal yr BP that was possibly connected with the intensification of typhoons although the storm activity in the archipelago was low. The period of paleo-typhoon activation in the south of Sakhalin Island occurred from 4640–4360 cal yr BP [75].

The frequency of severe storms occurred from 4280 to 3880 cal yr BP (phase 9) and included two subphases 4275–4140 cal yr BP, and 4010–3880 cal yr BP. During this time climatic conditions on the islands were warm. Bioaerosols included diatoms typical for both bays and the open sea. The main emission of marine bioaerosols occurred at a short distance from the island. Species transferred from the shallow part of the sea and the lagoon dominate in the peat. It is noteworthy that most of the diatom valves are intact and many large valves were found. This preservation is possibly explained by the large thickness of the valve walls of dominant species *Cocconeis costata*.

During this warming period, the water in the peat bog increased. Presence of allochthonous freshwater diatoms indicates that floods began to occur more frequently in the final stage of warming (4140–3360 cal yr BP). It is possible that the frequency of southern and southwestern cyclones increased. This is close to the period of active typhoons in South Sakhalin from 4030–3580 cal yr BP [75]. The warm subperiod from 4300–3550 cal yr BP in the southern part of the sea was associated with relatively strong intensity of the warm current [73].

From 3300–3000 cal yr BP, climatic conditions in the Okhotsk Sea region became cooler [73,76,77]. This coincides with the beginning of the neoglacial and the expansion of glaciers throughout the world (3003–2400 cal yr BP) [78]. In the Shantar area, high storm activity was observed from 2960–2570 cal yr BP (phase 10), coinciding with one of the well-pronounced Holocene global cold events [64]. Even a slight intensification of the warm Kuroshio Current from 2800–2400 yrs ago did not affect the climate of the Okhotsk Sea [73]. The abundance of neritic and oceanic species of diatoms in the studied peat bog shows that valves were captured during strong waves in the open sea. Around the Shantar Islands, ice appeared earlier in shallow water, preventing the development of waves in the autumn-winter season in the coastal areas.

Frequent storms in the marine areas and in the lagoons were recorded from 2570 to 1820 cal yr BP (phase 11) under warming conditions [66], specifically during 2570–2450 cal yr BP and 2200–2070 cal yr BP. More active removal of diatoms from the open sea during 2200–2070 cal yr BP possibly corresponds to a slight cooling. The wetness of the bog decreased from 2200 to 2070 cal yr BP [22].

The high concentration of marine diatoms, represented exclusively by neritic and oceanic species, indicates an increase in storm activity from 1570–1320 cal yr BP (phase 12). This period also corresponds to a global cold event during 1500–1300 cal yr BP [64]. Cold signals occurring at 1400 cal yr BP were also recorded by an increase in near-ice diatoms in the western part of the Okhotsk Sea [43]. The ice coverage around the Shantar Islands impeded the development of waves in the autumn-winter season; the removal of marine bioaerosols was, therefore, carried out from open sea. The increase in the intensity of southern winter cyclones, according to the peak of dwarf pine pollen, was from 1570–1440 cal yr BP [22].

Increased storm activity occurring from 820–570 cal yr BP (phase 13) was likely associated with the restructuring of the climatic system at the end of the Medieval Warm period and the beginning of the Little Ice Age. The first phase of the Little Ice Age in the Amur basin was colder [79]. The area of sea-water closest to the islands were frozen; therefore, the emission of marine bioaerosols proceeded mainly from the open sea. During 640–570 cal yr BP mainly deep-sea species were removed from the record.

In historical times, storm activity was much lower. The sea aerosols that arrived on the island took place in the 16th century (430–360 cal yr BP, phase 14) and from the second half of 20th century (phase 15). Phase 14 is associated with the activation of marine cyclones during restructuring during climatic fluctuations of the Little Ice Age, while phase 15 is associated with the change in the climatic regime to modern global warming. A sharp increase in the number of southern cyclones over the Okhotsk Sea during the cold period was noted in the second half of the 1980s to- mid-1990s [80,81].

Pollen peaks from fir and pine indicate an increase in the frequency of southwestern cyclones in the first half of the vegetation season from 4010–3880 cal yr BP and 3360–3220 cal yr BP. The first period coincides with the period of storm activity, but the second period does not. In the Late Holocene, the amount of broadleaf pollen sharply decreased. The Shantar region received only oak pollen (3750–3490, 3090–2960 cal yr BP). Individual strong floods during 3620–3490 cal yr BP [22] reflect the activation of southern cyclones. From 2960 cal yr BP, the influx of broadleaf pollen stopped and this is associated with a shift in the northern border of broadleaf distribution in the Lower Amur Region [37]. This time period (2800–2600 cal yr BP) also has one of the most extreme cold events in the Holocene [64].

From 1950 to 640 cal yr BP, the supply of fir pollen with bioaerosols increased to the islands and the supply of pine pollen slightly decreased. At the beginning of summer, continental western-southwestern cyclones became more active. A particularly active supply of *Abies* pollen was noted from 1950 to 1820 cal yr BP, which corresponds to a short-term cooling and drying recorded from 1950 to1800 cal yr BP in Sakhalin Island [74]. The active import of *Abies* pollen occurred in the Medieval Warm period from 1070 to 820 cal yr BP. During the climatic system that changed from warmer to cooler conditions at the beginning and end of the Little Ice Age (710–640, 500–430, 220–70 cal yr BP), cyclones of southwestern, western and northwestern directions became more active; fir and pine pollen began to flow more actively with winds.

5.4. Typical Changes in Atmosphere Circulation Affecting Bioaerosol Transport

Distribution of allochthonous diatoms and pollen in the peat bog section on Bolshoy Shantar Island provides information on atmospheric circulation anomalies in the autumn-winter season and during the restructuring from winter to summer circulation. Modern and paleo-oceanological data for the Late Glacial and the Holocene show that the winter atmospheric circulation in the Okhotsk Sea region, as well as its ice extent, largely depends on the geographical position of the two atmospheric centers of action: the Siberian High and the Aleutian Low [14,43,67,70,77].

In the late Glacial–Holocene, as well as the modern period during the 20th and early 21st centuries [82–84], the position of the Siberian High and the Aleutian Low underwent long-term fluctuations with many associated changes in atmospheric and ocean circulation. Changes in the centers of action of the atmosphere are accompanied by changes in

atmospheric fronts, the intensity of cyclogenesis, cyclones tracks, and the recurrence of extreme weather phenomena, including storms and precipitation. In the Late Glacial period (up to 10,000 cal yrs BP), with strengthening of the Siberian High and its displacement to the south, the strong winds of the western-northwestern points led to the formation of a polynya in the northern part of the Okhotsk Sea [67].

In the radiolarian data from Itaki and Ikehara [77], the periods of intensification (7500–3500 cal yr BP) and weakening (3000–2000, 400–300 cal yr BP) of intermediate ventilation of Okhotsk Sea waters were caused by significant changes in atmospheric circulation. During the warm period (7500–3500 cal yr BP), the Aleutian Low shifted northward and northern winds from Siberia dominated [84], contributing to the development of an extensive polynya in the western part of the sea, including the waters the Shantar Islands. It is possible that one of the signs of aerosol emission from the polynya is the presence of diatoms attached to the ice or living near the ice edge. Such species were carried with aerosols until 6810 cal yr BP and in recent decades. From 5000 to 3000 cal yr BP, there was a gradual intensification of the Siberian High [39]. During cold periods (3000–2000 cal yr BP, 400–300 cal yr BP), the Aleutian Low intensified and shifted to the south-southwest leading to an increase in the role of eastern winds, which caused more intensive increase in ice coverage that contributed to the closure of the polynya [77]. The Aleutian Low shifting to the southwest and the Siberian High strengthening in the Late Holocene led to an intensification of cyclonic circulation along the Siberian storm track east of Kamchatka with the development of constant northeastern winds and increased winter precipitation [39].

The effect of strengthening storms on the transfer of bioaerosols, identified by the presence of marine diatoms in the Shantar peat bog section typical for the autumn season, coincided well with the periods of intensification of southern cyclones in the cold season, which were shown by an increase in dwarf pine pollen (Figure 6). As in modern conditions [81], the frequency and intensity of cyclones entering the Okhotsk Sea during the cold season in the Holocene likely increased during the western displacement of the Siberian High and the Aleutian Low.

The decreased background pressure over the Okhotsk Sea led to the strengthening of cyclogenesis, which was more active than in the Japan Sea [50]. Southern cyclones caused southern winds to increase, facilitated warm air penetration and, to some extent, could have reduced ice coverage in this part of the Okhotsk Sea [81]. Cyclogenesis was facilitated by the large temperature contrast between the continent and the ocean [80]. The recurrence of cyclones in the Okhotsk Sea occur most often in December, when the temperature contrast between the mainland and the Far Eastern seas is especially great [85]. Most recurrences of extreme storms in the past (Figure 6) coincided with cold events identified for the Okhotsk Sea [65]. It is possible that during cold periods the temperature contrast between the sea and the continent is larger and contributes to a more intense cyclogenesis.

The intensification phases of continental cyclones entering the Okhotsk Sea in the spring-summer season coincided with various periods of increased cyclogenesis in the cold season. There are also phases of cyclone intensification from the continent, and with cyclonic activity decrease in the winter season.

Under modern warming conditions, the number of southern cyclones entering the Okhotsk Sea in the cold season decreases, but their intensity increases [83]. The warm season is characterized by decreased pressure and an increase in the Asian and Far Eastern Low, accompanied by increased pressure over the ocean (active state of the North Pacific High). In general, cyclogenesis weakening over the region is observed, but cyclones reaching the Okhotsk Sea have the highest intensity. The intensity of western continental cyclones also increases, coming from areas of continental lows, which leads to an increase in the transfer of warm air from the south [83].

In the modern period (20th–early 21st centuries), as well as on the paleoscale, there are multi-year and centuries-old periods when the number and intensity of cyclones in Northeast Asia and the northwestern Pacific [86] increases or decreases [83,87]. Cyclonic activity over the Okhotsk Sea is mainly determined by extratropical cyclones that emerge

from the west and southwest and less often from tropical cyclones that emerge from the south or southwest. The emergence of deep cyclones occurs with an increase in temperature contrasts over the continent and the sea and with the structure of the baric field when it is favorable for the development of a cyclonic vortex. Such conditions are created when a cyclone passes through the Amur basin to the Okhotsk Sea, followed by an intense cold pattern in Eastern China and the Yellow Sea [50]. The passage of the western cyclone is usually accompanied by prolonged penetration of cold continental air to the south Far East. Therefore, the cyclogenetic conditions persist here for long periods, until the zonal process develops again over the temperate latitudes of East Asia. In the presence of polynyas during winter, cyclones around the Okhotsk Sea intensify, and in summer over the open sea surface, they intensify further. The activation of the summer cyclonic circulation over both the continent and sea regions of the Far East is observed with the displacement of the high-altitude ridge to Kamchatka and the high-altitude Siberian trough to Yakutia and the Amur basin.

The intensity and the number of continental and marine cyclones moving along different tracks to the Okhotsk Sea or adjacent areas of the Japan Sea [61] change from year to year and over longer time periods [83,87], depending on the synoptic characteristics of these periods, as well as anomalies of the centers of action of the atmosphere, which contribute to the strengthening or weakening of cyclogenesis in Northeast Asia, the northwestern Pacific Ocean and marginal seas. The atmospheric circulation over the Sea of Okhotsk in the winter season is also influenced by the tropospheric cyclone identified on average monthly maps by the H500mb geopotential height [88]. Extremely low air temperatures over the coast of northeastern Asia are related with this cyclone development over the Okhotsk Sea. Long-term data show that the depth of this cyclone varies from year to year during the winter months, and likely changed during the Holocene, as shown by the example of the Aleutian Low.

The periods with established strong winds around the Shantar Islands agree well (Figure 6) with natural wind cycles recorded by dust flux in ice cores within Dome C, Antarctica [62]. This confirms that paleoscale Antarctic Oscillation was accompanied by similar alternation of cold and warm periods in the northern hemisphere during the Holocene.

6. Conclusions

The 15 phases of increased storm activity for the last 12.5 ka were analyzed, when marine bioaerosols with marine diatoms were carried to the peat bog on Bolshoy Shantar Island. It is assumed that the main extreme storms took place in the autumn-winter season and were associated with the passage of deep cyclones over the sea. The composition of bioaerosols differs markedly between cold and warm periods. In cold periods (phases 8, 10, 12 and the end of the 13th), the emission of bioaerosols came from the open sea at great distances from the island. In this case, mainly oceanic and neritic diatoms were captured in the aerosols. The adjacent coastal waters were covered with ice, shielding the effect of storm wind on the shelf waters. During warm periods (phases 6, 9, 11), the main emission of bioaerosols took place in nearby coastal waters. Bioaerosols consisted mainly of sublittoral species inhabiting open bays, freshened shallow seawater and lagoons. The main emission of bioaerosols took place during strong wind gusts when waves were breaking. In the early Holocene, marine diatoms could also have been redeposited from the drained shelf. In the Middle Holocene, when the sea level reached its present position and even exceeded it, the supply of marine diatoms came only from the sea. Diatoms living on the ice sheet or near the ice edge are found only from 6810 cal yr BP until recent decades.

The most intense phases of storm activity were associated with significant changes in atmospheric circulation during the transition from warming to cooling, and coincide with cold events. The presence of marine diatoms, an increase in dwarf pine pollen and stable snow cover showed periods of increased frequency of cyclones in the Shantar Island region during the cold season. The longest periods of cyclogenesis increase were from 9200 to 6440 cal yr BP (phases 3–6) and 2960 to 1820 cal yr BP (phases 10–11).

The presence of allochthonous pollen is evidence of an increase in the frequency of continental cyclones at the beginning of the growing season, i.e., when winter circulation changes to summer. The most distant transfer of broadleaf pollen took place in the Younger Dryas–Early Holocene with southern cyclones. In the Holocene, an increase in pine pollen indicates western and northwestern cyclones, fir—western and southwestern, broad-leaved—southwestern and southern. Periods of intensification of continental cyclones over the northwestern Okhotsk Sea and Shantar Islands in summer coincide with periods of intensification of winter cyclogenesis in the late Glacial–Holocene.

Supplementary Materials: The following supporting information can be downloaded at: https://www.mdpi.com/article/10.3390/cli10020024/s1, Table S1: List of marine diatom species from peat bog of Bolshoy Shantar Island.

References

1. Fröhlich-Nowoisky, J.; Kampf, C.J.; Weber, B.; Huffman, J.A.; Pöhlker, C.; Andreae, M.O.; Lang-Yona, N.; Burrows, S.M.; Gunthe, S.S.; Elbert, W.; et al. Bioaerosols in the Earth system: Climate, health, and ecosystem interactions. *Atmos. Res.* **2016**, *182*, 346–376. [CrossRef]
2. Borodulin, A.I.; Safatov, A.S.; Belan, B.D.; Panchenko, M.V. The height distribution and seasonal variations of the tropospheric aerosol biogenic component concentration on the south of western Siberia. *J. Aerosol Sci.* **2003**, *34*, 681.
3. Manninen, H.E.; Back, J.; Sihto-Nissila, S.L.; Huffman, J.A.; Pessi, A.M.; Hiltunen, V.; Aalto, P.P.; Hidalgo, P.J.; Hari, P.; Saarto, A.; et al. Patterns in airborne pollen and other primary biological aerosol particles (PBAP), and their contribution to aerosol mass and number in a boreal forest. *Boreal Environ. Res.* **2014**, *19*, 383–405.
4. Rogers, C.A.; Levetin, E. Evidence of long-distance transport of mountain cedar pollen into Tulsa, Oklahoma. *Int. J. Biometerol.* **1998**, *42*, 65–72. [CrossRef]
5. Misaki, K. Aerosol Behavior. *Kise Kenkyu Noto* **1981**, *142*, 95–182. (In Japanese)
6. Kondrat'ev, I.I. *Transboundary Atmospheric Transport of Aerosol and Acid Precipitation to the Russian Far East*; Dalnauka: Vladivostok, Russia, 2013. (In Russian)
7. Hoose, C.; Kristjansson, J.E.; Burrows, S.M. How important is biological ice nucleation in clouds on a global scale? *Environ. Res. Lett.* **2010**, *5*, 024009. [CrossRef]
8. Möhler, O.; DeMott, P.J.; Vali, G.; Levin, Z. Microbiology and atmospheric processes: The role of biological particles in cloud physics. *Biogeosciences* **2007**, *4*, 1059–1071. [CrossRef]
9. Pope, F.D. Pollen grains are efficient cloud condensation nuclei. *Environ. Res. Lett.* **2010**, *5*, 044015. [CrossRef]
10. Steiner, A.L.; Brooks, S.D.; Deng, C.; Thornton, D.C.; Pendleton, M.W.; Bryant, V. Pollen as atmospheric cloud condensation nuclei. *Geophys. Res. Lett.* **2015**, *42*, 3596–3602. [CrossRef]
11. Mikhailov, E.F.; Ivanova, O.A.; Nebosko, E.Y.; Vlasenko, S.S.; Ryshkevich, T.I. Subpollen particles as atmospheric cloud condensation nuclei. *Izv. Atmos. Ocean. Phys.* **2019**, *55*, 357–364. [CrossRef]

12. Taylor, P.E.; Flagan, R.C.; Miguel, A.G.; Valenta, R.; Glovsky, M.M. Birch pollen rupture and the release of aerosols of respirable allergens. *Clin. Exp. Allergy* **2004**, *34*, 1591–1596. [CrossRef] [PubMed]

13. Petrov, E.S.; Novorotskiy, P.V.; Lenshin, V.T. *The Climate of the Khabarovsky Krai and the Jewish Autonomous Region*; Dalnauka: Khabarovsk, Russia, 2000. (In Russian)

14. Kimura, N.; Wakatsuchi, M. Increase and decrease of sea ice are in the Sea of Okhotsk: Ice production in coastal polynyas and dynamic thickening in convergence zones. *J. Geophys. Res.* **2004**, *109*, C09S03. [CrossRef]

15. Rogachev, K.A. Satellite observations of regular whirl winds in the bays of the Shantarsky Archipelago, Sea of Okhotsk. *Issled. Zemli Iz Kosm.* **2012**, *1*, 54–60. (In Russian)

16. Rogachev, K.A.; Shlyk, N.V. Jet flow of the Shantarsky Archipelago: Satellite data. *Issled. Zemli Iz Kosm.* **2014**, *5*, 68–75. (In Russian)

17. Terziev, F.S. (Ed.) *Hydrometeorology and Hydrochemistry of the Seas. T. IX. Sea of Okhotsk. Issue 1. Hydrometeorological Conditions*; Hydrometeoizdat: St. Petersburg, Russia, 1998. (In Russian)

18. Kulakov, A.P. *Quaternary Coastal Lines of Okhotsk and Japan Seas*; Nauka: Novosibirsk, Russia, 1973. (In Russian)

19. Ganeshin, V.G. Origin of the Shantarskie Islands. *Priroda* **1956**, *4*, 91–93. (In Russian)

20. Zhabin, I.A.; Luk'yanova, N.B.; Dubina, V.A. The Water Structure and Dynamics of the Shantar Islands National Park Aquatory (the Sea of Okhotsk) According to Satellite Data. *Issled. Zemli Iz Kosm.* **2018**, *5*, 3–14. [CrossRef]

21. Shlotgauer, S.D.; Kryukova, M.V. Vegetation cover of the Shantarskie Islands. *Geogr. Nat. Resour.* **2012**, *3*, 110–114. (In Russian)

22. Razjigaeva, N.G.; Grebennikova, T.A.; Ganzey, L.A.; Chakov, V.V.; Klimin, M.A.; Mokhova, L.M.; Zakharchenko, E.N. The stratigraphy of the blanket peatland and the development of environments on Bolshoi Shantar Island in the Late Glacial–Holocene. *Russ. J. Pac. Geol.* **2021**, *15*, 252–267. [CrossRef]

23. Blaauw, M.; Christen, J.A. Flexible paleoclimate age-depth models using an 601 autoregressive gamma process. *Bayesian Anal.* **2011**, *6*, 457–474. [CrossRef]

24. Gleser, Z.I.; Jousé, A.P.; Makarova, I.V.; Proshkina-Lavrenko, A.I.; Sheshukova-Poretskaya, V.S. (Eds.) *Diatom Algal of the USSR. Fossil and Recent*; Nauka: Leningrad, Russia, 1974; Volume 1. (In Russian)

25. Battarbee, R.W. Diatom analysis. In *Handbook of Holocene Paleoecology and Paleohydrology*; Berglund, B.E., Ed.; Wiley & Sons: London, UK, 1986; pp. 527–570.

26. Jouse, A.P. *Atlas of Microorganisms in Ocean Bottom Sediments. Diatoms, Radiolarians, Silicoflagellates, Coccoliths*; Nauka: Moscow, Russia, 1977. (In Russian)

27. Loseva, E.I. *Atlas of Marine Pleistocene Diatoms of European North-West of USSR*; Nauka: St. Peterburg, Russia, 1992. (In Russian)

28. Tsoy, I.B.; Obrezkova, M.S. *Atlas of Diatom Algae and Silicoflagellates from Holocene Sediments of the Russian East Arctic Seas*; POI FEB RAS Publ.: Vladivostok, Russia, 2017. (In Russian)

29. Pokrovskaya, I.M. Methods of paleopollen studies. In *Paleopalynology*; Pokrovskaya, I.M., Ed.; Nedra: Leningrad, Russia, 1966; pp. 29–60. (In Russian)

30. Kharkevich, S.S. (Ed.) *Vascular Plants of the Soviet Far East*; Nauka: Moscow, Russia, 1989; Volume 4. (In Russian)

31. Takhtajan, A.L. *Floristic Areas of the Earth*; Nauka: Leningrad, Russia, 1978. (In Russian)

32. Kharkevich, S.S. (Ed.) *Vascular Plants of the Soviet Far East*; Nauka: Moscow, Russia, 1991; Volume 5. (In Russian)

33. Kharkevich, S.S. (Ed.) *Vascular Plants of the Soviet Far East*; Nauka: Moscow, Russia, 1996; Volume 8. (In Russian)

34. Kharkevich, S.S. (Ed.) *Vascular Plants of the Soviet Far East*; Nauka: Moscow, Russia, 1987; Volume 2. (In Russian)

35. Korotky, A.M.; Pletnev, S.P.; Pushkar, V.S.; Grebennikova, T.A.; Razzhigaeva, N.G.; Sakhebgareeva, E.D.; Mokhova, L.M. *Development of Natural Environments of South Far East (the Late Pleistocene-Holocene)*; Nauka: Moscow, Russia, 1988. (In Russian)

36. Korotky, A.M.; Grebennikova, T.A.; Pushkar, V.S.; Razzhigaeva, N.G.; Volkov, V.G.; Ganzey, L.A.; Mokhova, L.M.; Bazarova, V.B.; Makarova, T.R. Climatic changes of the territory of South Far East at Late Pleistocene-Holocene. *Bull. FEB RAS* **1997**, *3*, 121–143. (In Russian)

37. Bazarova, V.B. Spreading of broadleaved species in Amur River basin in the Holocene. *Bot. Pac.* **2014**, *3*, 47–54. [CrossRef]

38. Anderson, P.M.; Lozhkin, A.V.; Solomatkina, T.B.; Brown, T.A. Paleoclimatic implications of glacial and postglacial refugia for *Pinus pumila* in Western Beringia. *Quat. Res.* **2010**, *73*, 269–276. [CrossRef]

39. Hammarlund, D.; Klimaschewski, A.; Amour, N.A.S.; Andrén, E.; Self, A.E.; Solovieva, N.; Andreev, A.A.; Barnekowa, L.; Thomas, W.D.; Edwards, T.W.D. Late Holocene expansion of Siberian dwarf pine (*Pinus pumila*) in Kamchatka in response to increased snow cover as inferred from lacustrine oxygen-isotope records. *Glob. Planet. Change* **2015**, *134*, 91–100. [CrossRef]

40. Sancetta, C. Oceanographic and ecologic significance of diatoms in surface sediments of the Bering and Okhotsk Seas. *Deep-Sea Res.* **1981**, *28A*, 789–817. [CrossRef]

41. Jouse, A.P. *Stratigraphic and Paleogeographic Studies in the Northwest Pacific*; Nauka: Moscow, Russia, 1962. (In Russian)

42. Sancetta, C. Distribution of diatom species in surface sediments of the Bering and Okhotsk seas. *Micropaleontology* **1982**, *28*, 221–257. [CrossRef]

43. Gorbarenko, S.A.; Psheneva OYu Artemova, A.V.; Matul, A.G.; Tiedemann, R.; Nürnberg, D. Paleoenvironment changes in the NW Okhotsk Sea for the last 18 thousand years by micropaleontologic, geochemical, and lithological data. *Deep-Sea Res.* **2010**, *57*, 797–811. [CrossRef]

44. Verkulich, S.R.; Pushina, Z.V.; Dorozhkina, M.V.; Melles, M.; Rethemeyer, J. Characterization of environmental conditions of the interstadial (MIS 3) deposits formation in King George Island (West Antarctica) based on the study of fossil diatom assemblages. *Probl. Arct. Antarct.* **2015**, *3*, 109–119. (In Russian)

45. Nair, A.; Mohan, R.; Shetye, S.; Gazi, S.; Jafar, S.A. *Trigonium curvatus* sp. nov. and *Trigonium arcticum* (Bacillariophyceae) from the surface sediments of Prydz Bay, East Antarctica. *Micropaleontology* **2015**, *61*, 185–192.

46. Kharitonov, V.G. *Synopsis of Diatom Flora (Bacillariophyceae) of Northern Okhotsk Sea Region*; NECSI FEB RAS Publ.: Magadan, Russia, 2010. (In Russian)

47. Makarova, I.V.; Strelnikova, N.I.; Kozyrenko, T.F.; Gladenkov, A.Y.; Jakovschikova, T.K.; Kazarina, G.K.; Nikolaev, V.A.; Potapova, M.G. (Eds.) *The Diatoms of Russia and Adjacent Countries: Fossil and Recent*; St.-Petersburg State University Publ.: St. Petersburg, Russia, 2002; Volume II. (In Russian)

48. Pushkar, V.S.; Cherepanova, M.V.; Likhacheva, O.Y. Detalization of the Pliocene-Quaternary North Pacific diatom zonal scale. *Algologia* **2014**, *24*, 94–117. [CrossRef]

49. Ryabushko, L.I. Diatoms (Bacillariophyta) of the Vostok Bay, Sea of Japan. *Biodivers. Environ. Far East Reserves* **2014**, *2*, 4–17. (In Russian)

50. Tunegolovets, V.P. The intensity of cyclogenesis in the second half of the twentieth century. *Izv. TINRO* **2009**, *151*, 140–153. (In Russian)

51. Sorokin, Y.I. Primary production in the Okhotsk Sea. In *Comprehensive Researches of Ecosystem of the Sea of Okhotsk*; Sapozhnikov, V.V., Ed.; VNIRO: Moscow, Russia, 1997; pp. 103–110. (In Russian)

52. Pishchalnik, V.M.; Bobkov, A.O. *Oceanographical Atlas of the Sakhalin Shelf*; Sakhalin State University: Yuzhno-Sakhalinsk, Russia, 2000. (In Russian)

53. Yokoyama, Y.; Esat, T.M. Global climate and sea level–enduring variability and rapid fluctuations over the past 150,000 years. *Oceanography* **2011**, *24*, 54–67. [CrossRef]

54. Golovko, V.V.; Koutsenogii, K.P.; Istomin, V.L. Number and mass concentrations of the pollen component of atmospheric aerosol measured near Novosibirsk during blossoming of arboreal plants. *Atmos. Ocean. Opt.* **2015**, *28*, 529–533. (In Russian) [CrossRef]

55. Bazarova, V.B.; Klimin, M.A.; Mokhova, L.M.; Orlova, L.A. New pollen records of Late Pleistocene and Holocene changes of environment and climate in the Lower Amur River basin, NE Eurasia. *Quat. Int.* **2008**, *179*, 9–19. [CrossRef]

56. Razzhigaeva, N.G.; Ganzey, L.A.; Mokhova, L.M.; Grebennikova, T.A.; Panichev, A.M.; Kopoteva, T.A.; Kudryavtseva, E.P.; Arslanov, K.A.; Maksimov, F.E.; Starikova, A.A.; et al. Stages of landscape evolution on the western macroslope of Sikhote-Alin at the Pleistocene–Holocene transition (Bikin River basin). *Geogr. Nat. Resour.* **2017**, *3*, 127–138. (In Russian)

57. Igarashi, Y.; Zharov, E. Climate and vegetation change during the late Pleistocene and early Holocene in Sakhalin and Hokkaido, northeast Asia. *Quat. Int.* **2011**, *237*, 24–31. [CrossRef]

58. Leipe, C.; Nakagawa, T.; Gotanda, K.; Müller, S.; Tarasov, P. Late Quaternary vegetation and climate dynamics at the northern limit of the East Asian summer monsoon and its regional and global-scale controls. *Quat. Sci. Rev.* **2015**, *116*, 57–71. [CrossRef]

59. Razjigaeva, N.G.; Ganzey, L.A.; Grebennikova, T.A.; Mokhova, L.M.; Kopoteva, T.A.; Kudryavtseva, E.P.; Belyanin, P.S.; Panichev, A.M.; Arslanov, K.A.; Maksimov, F.E.; et al. Holocene mountain landscape development and monsoon variation in the southernmost Russian Far East. *Boreas* **2021**, *50*, 1043–1058. [CrossRef]

60. Li, C.; Wu, Y.; Hou, X. Holocene vegetation and climate in Northeast China revealed from Jingbo Lake sediment. *Quat. Int.* **2011**, *229*, 67–73. [CrossRef]

61. Mezentseva, L.I.; Grishina, M.A.; Kondrat'ev, I.I. Trajectories and depth of cyclones entering Primorsky Krai. *Bull. FEB RAS* **2019**, *3*, 121–143. (In Russian)

62. Davis, W.J.; Davis, W.B. Antarctic winds: Pacemaker of global warming, global cooling, and the collapse of civilizations. *Climate* **2020**, *8*, 130. [CrossRef]

63. Steinhilber, F.; Beer, J.; Fröhlich, C. Total solar irradiance during the Holocene. *Geophys. Res. Lett.* **2009**, *36*, L19704. [CrossRef]

64. Wanner, H.; Solomina, O.; Grosjean, M.; Ritz, S.P.; Jetel, M. Structure and origin of Holocene cold events. *Quat. Sci. Rev.* **2011**, *30*, 3109–3123. [CrossRef]

65. Gorbarenko, S.A.; Artemova, A.V.; Goldberg, E.L.; Vasilenko, Y.P. The response of the Okhotsk Sea environment to the orbital-millennium global climate changes during the Last Glacial Maximum, deglaciation and Holocene. *Glob. Planet. Change* **2014**, *116*, 76–90. [CrossRef]

66. Khotinsky, N.A. *Holocene of Northern Eurasia*; Nauka: Moscow, Russia, 1977. (In Russian)

67. Katsuki, K.; Khim, B.-K.; Itaki, T. Sea-ice distribution and atmospheric pressure patterns in southwestern Okhotsk Sea since the Last Glacial Maximum. *Glob. Planet. Change* **2010**, *72*, 99–107. [CrossRef]

68. Korotkii, A.M. Quaternary sea-level fluctuations on the Northwestern shelf of the Japan Sea. *J. Coast. Res.* **1985**, *1*, 293–298.

69. Pushkar, V.S.; Cherepanova, M.V. *Diatom Assemblages and Correlation of Quaternary Deposits of the Northwestern Pacific Ocean*; Dalnauka: Vladivostok, Russia, 2008. (In Russian)

70. Harada, N.; Katsuki, K.; Nakagawa, M.; Matsumoto, A.; Seki, O.; Addison, J.A.; Finney, B.P.; Sato, M. Holocene sea surface temperature and sea ice extent in the Okhotsk and Bering Seas. *Prog. Oceanogr.* **2014**, *126*, 242–253. [CrossRef]

71. Bazarova, V.B.; Klimin, M.A.; Kopoteva, T.A. Holocene dynamic of Eastern-Asia Monsoon in Lower Amur Area. *Geogr. Nat. Resour.* **2018**, *39*, 124–133. [CrossRef]

72. Chen, R.; Shen, J.; Li, C.; Zhang, E.; Sun, W.; Ji, M. Mid- to late-Holocene East Asian summer monsoon variability recorded in lacustrine sediments from Jingpo Lake, Northeastern China. *Holocene* **2015**, *25*, 454–468. [CrossRef]

73. Kawahata, H.; Ohshima, H.; Shimada, C.; Oba, T. Terrestrial oceanic environmental change in the southern Okhotsk Sea during the Holocene. *Quat. Int.* **2003**, *108*, 67–76. [CrossRef]

74. Mikishin, Y.A.; Gvozdeva, I.G. Early-Middle Holocene of Northern Sakhalin. *Bull. NESC FEB RAS* **2021**, *1*, 50–65. [CrossRef]
75. Razjigaeva, N.G.; Grebennikova, T.A.; Ganzey, L.A.; Ponomarev, V.I.; Gorbunov, A.O.; Klimin, M.A.; Arslanov, K.A.; Maksimov, F.E.; Petrov, A.Y. Recurrence of extreme floods in south Sakhalin Island as evidence of paleo-typhoon variability in North-Western Pacific since 6.6 ka BP. *Palaeogeogr. Palaeoclimatol. Palaeoecol.* **2020**, *556*, 109901. [CrossRef]
76. Korotky, A.M.; Razjigaeva, N.G.; Grebennikova, T.A.; Ganzey, L.A.; Mokhova, L.M.; Bazarova, V.B.; Sulerzhitsky, L.D.; Lutaenko, K.A. Middle and Late Holocene environments and vegetation history of Kunashir Island, Kurile Islands, northwestern Pacific. *Holocene* **2000**, *11*, 311–331. [CrossRef]
77. Itaki, T.; Ikehara, K. Middle to late Holocene changes of the Okhotsk Sea Intermediate Water and their relation to atmospheric circulation. *Geophys. Res. Lett.* **2004**, *31*, L24309. [CrossRef]
78. Denton, G.H.; Karlen, W. Holocene climatic variations. Their pattern and possible cause. *Quat. Res.* **1973**, *3*, 155–205. [CrossRef]
79. Bazarova, V.B.; Grebennikova, T.A.; Orlova, L.A. Natural-environment dynamics within the Amur basin during the neoglacial. *Geogr. Nat. Resour.* **2014**, *35*, 275–283. [CrossRef]
80. Tunegolovets, V.P.; Kochetkova, M.V.; Cherednichenko, U.A. Climatic generalizations of southern cyclones entering the Far Eastern seas and the northwestern part of the Pacific Ocean during the cold season. *Izv. TINRO* **2009**, *151*, 109–126. (In Russian)
81. Glebova, S.Y. Fall-winter cyclogenesis over the Pacific Ocean and Far-Eastern Seas and its influence on development of the sea ice. *Izv. TINRO* **2017**, *191*, 147–159. [CrossRef]
82. Parkinson, C.L. The impact of the Siberian high and Aleutian low on the sea-ice cover of the Sea of Okhotsk. *Ann. Glaciol.* **1990**, *14*, 226–229. [CrossRef]
83. Glebova, S.Y. Cyclones over the Pacific Ocean and Far-Eastern Seas in cold and warm seasons and their influence on wind and thermal regime in the last two decade period. *Izv. TINRO* **2018**, *193*, 153–166. [CrossRef]
84. Martin, S.; Drucker, R.; Yamashita, K. The production of ice and dense shelf water in the Okhotsk Sea polynyas. *J. Geophys. Res.* **1998**, *103*, 771–782. [CrossRef]
85. Il'insky, O.K.; Egorova, M.V. Cyclonic activity over the Okhotsk Sea during cold half year. *Tr. FERHRI* **1962**, *14*, 34–38. (In Russian)
86. Zhang, Y.; Ding, Y.; Li, Q. A climatology of extratropical cyclones over East Asia during 1958–2001. *Acta Meteorol. Sin.* **2012**, *26*, 261–277. [CrossRef]
87. Mesquita, M.D.S.; Hodges, K.I.; Bader, J. Sea-ice anomalies in the Sea of Okhotsk and the relationship with storm tracks in the Northern Hemisphere during winter. *Tellus* **2011**, *63*, 312–323. [CrossRef]
88. Shatilina, T.A.; Tsitsiashvili, G.S.; Radchenkova, T.V. The Okhotsk tropospheric cyclone and its role in the occurrence of extreme air temperature in January in 1950–2019. *Izv. TINRO* **2021**, *201*, 64–79. [CrossRef]